Frequency Domain DTV Pilot Detection Based on the Bussgang Theorem for Cognitive Radio

Sung Sue Hwang, Dong Chan Park, and Suk Chan Kim

In this paper, a signal detection scheme for cognitive radio (CR) based on the Bussgang theorem is proposed. The proposed scheme calculates the statistical difference between Gaussian noise and the primary user signal by applying the Bussgang theorem to the received signal. Therefore, the proposed scheme overcomes the noise uncertainty and gives scalable complexity according to the zero-memory nonlinear function for a mobile device. We also present the theoretical analysis on the detection threshold and the detection performance in the additive white Gaussian noise channel. The proposed detection scheme is evaluated by computer simulations based on the IEEE 802.22 standard for the wireless regional area network. Our results show that the proposed scheme is robust to the noise uncertainty and works well in a very low signal-to-noise ratio.

Keywords: Cognitive radio, Bussgang theorem, DTV signal detection, pilot.

I. Introduction

Efficient utilization of the spectrum resource that is already allocated has become the most important issue in the wireless communication field. According to a report by the Federal Communications Commission (FCC), the spectrum is not efficiently utilized since the assigned spectrum to the existing wireless communication systems is not used in a specific time and area [1]. To enhance the spectrum efficiency, the FCC has permitted the secondary systems to use a licensed spectrum opportunistically under the condition that there is no interference from the secondary systems that affects the primary systems.

Cognitive radio (CR) is the wireless communication technology that senses a surrounding radio environment. CR has been considered the effective technology to implement opportunistic and efficient use of spectrum [2]. IEEE formed the 802.22 working group for wireless regional area network (WRAN) standardization that enables rural broadband wireless access using CR technology in TV white spaces [3]. The most important challenge of IEEE 802.22 WRAN's technical requirement is the accurate sensing algorithm that can detect the DTV signal at a very low signal-to-noise ratio (SNR) since the fundamental condition of WRAN prevents interference in the licensed system. To satisfy the sensing scheme requirement of WRAN, many kinds of sensing schemes have been proposed [4]. Conventional sensing schemes utilize various characteristics of the primary user signal (PUS), and each scheme has its own advantages and disadvantages. Common problems of sensing schemes can be summarized as the detection performance, the noise uncertainty, and the computational complexity. One of the conventional detection schemes, the energy detection [5]-[7] is a very simple scheme

Manuscript received Aug. 21, 2012; revised Dec. 28, 2012; accepted Jan. 11, 2013.
Parts of this work were presented at the IEEE Milcom conference, in 2008.
This work was supported by the Industrial Strategic technology development program, No. 10041947 funded by the Ministry of Knowledge Economy (MKE, Korea)
Sung Sue Hwang (phone: +82 51 510 1394, sshwang@sk.com) is with the Department of Electronic Engineering, Pusan National University, Busan, Rep. of Korea, and also with the HMI Tech. Lab, Seoul, Rep. of Korea.
Dong Chan Park (dongchan@pusan.ac.kr) and Suk Chan Kim (corresponding author, sckim@pusan.ac.kr) are with the Department of Electronic Engineering, Pusan National University, Busan, Rep. of Korea.
http://dx.doi.org/10.4218/etrij.13.0112.0556

and it can detect the PUS without prior knowledge. However, the detection performance of the energy detection is highly related to the noise uncertainty [8]-[10] because the energy detection needs the noise power estimation. When perfect knowledge of PUS is available, the matched-filtering detection [7], [11], [12] is an optimal detection method; however, it does not work well with partial knowledge. The cyclostationary-based detection utilizes the cyclic frequency of the PUS [12]-[16]. It performs well when the SNR is very low, but it costs considerable computational complexity. Covariance-based detection [17] and eigenvalue-based detection [18] can overcome the noise uncertainty, but the detection performance is insufficient at low SNR. To overcome the referred problems, we propose a new signal detection scheme based on the Bussgang theorem [19], [20].

The Bussgang theorem has been used in various fields (for example, adaptive equalization and analysis on the nonlinear channel effect). The theorem states that the ratio of the autocorrelation of a real Gaussian stationary process with zero mean to the cross-correlation of the process and the distorted version of the process by a zero-memory nonlinear function (ZMNF) becomes a proportionality constant that is determined only by the ZMNF. By applying the Bussgang theorem to the received signal, the proposed scheme can detect PUS by the calculation of the difference between the PUS's proportionality constant and the Gaussian noise's proportionality constant. A similar approach is used for the Gaussianity test of the stationary series [21]. In this paper, we use this approach for the detection of the DTV signal, which is the PUS for WRAN. The proposed scheme is applied to the DTV signal in the frequency domain for the pilot detection since the DTV signal is close to a Gaussian process in the time domain. There are conventional research works that utilize the DTV pilot tone for more accurate detection [22]-[25], and they show that the use of the DTV pilot tone gives SNR gain for the energy detection. When the detection scheme based on the Bussgang theorem is applied to the DTV signal in the frequency domain, we can expect better detection performance because of the SNR gain and the nonstationary characteristic given by the pilot tone. Furthermore, we present the theoretical threshold and the DTV detection performance in the additive white Gaussian noise (AWGN) channel with a frequency domain pilot model. The proposed method is evaluated by computer simulations with the generated DTV signal and the captured DTV signal [26].

This paper is organized as follows. In section II, we briefly review the background for the spectrum-sensing system model and the Bussgang theorem. The proposed detection algorithm for the DTV signal detection is described in section III. In section IV, analysis of the theoretical threshold and the detection probability of the proposed scheme is provided. Simulation results that demonstrate the sensing performance of the proposed method are presented in section V. Finally, conclusions are given in section VI.

II. Sensing Model and Bussgang Theorem

1. Sensing Model

The aim of the detection problem is to distinguish between the two hypotheses (H_0: PUS is absent; H_1: PUS is present). Under the two hypotheses, the respective received signals $r[n]$ through a single sensor with a single receiver are described as follows:

$$H_0 : r[n] = w[n], \tag{1}$$

$$H_1 : r[n] = s[n] * g[n] + w[n], \tag{2}$$

where $s[n]$ denotes the PUS, $g[n]$ is the channel impulse response from the primary user to the secondary user, $w[n]$ represents the complex AWGN with $\mathcal{CN}(0, \sigma_n^2)$, and $*$ represents the convolution operator. The performance measures of the sensing scheme are the detection probability P_D and the false alarm probability P_{FA}. The detection probability P_D under H_1 is represented as

$$P_D = P[T \geq \lambda \mid H_1], \tag{3}$$

where T denotes the test statistic of the detection scheme and λ is the detection threshold. The false alarm probability P_{FA} under H_0 is described as

$$P_{FA} = P[T \geq \lambda \mid H_0]. \tag{4}$$

A substantial sensing algorithm requires higher P_D and lower P_{FA} in a low SNR simultaneously, but there is a tradeoff between P_{FA} and P_D.

2. Bussgang Theorem

The Bussgang theorem states that when a real Gaussian stationary process with zero mean passes through a ZMNF, the cross-correlation of input and output is proportional to the autocorrelation of input, that is,

$$C = \frac{E\{x[n] \cdot V(x[n+\tau])\}}{E\{x[n] \cdot x[n+\tau]\}}, \tag{5}$$

where $x[n]$ is the real Gaussian stationary process with $\mathcal{N}(0, \sigma_x^2)$, $V(\cdot)$ denotes the ZMNF, τ represents a time delay, $E\{\cdot\}$ represents the statistical mean, and C is the proportionality constant. The theoretical proportionality constant is not a function of the time delay. It can be rewritten as follows [19]:

$$C = \frac{1}{\sigma_x^3 \sqrt{2\pi}} \int_{-\infty}^{\infty} x \cdot V(x) e^{-x^2/2\sigma_x^2} dx. \quad (6)$$

The proportionality constant is determined by σ_x^2 and the ZMNF. As the Bussgang theorem only holds for a stationary real Gaussian process, it can also be used for signal detection since the Bussgang theorem does not hold for the PUSs. In this paper, we utilize the difference between the theoretical proportionality C and the sample proportionality constant of the received signal for the signal detection.

III. Proposed Detection Scheme

There are several types of PUSs for the IEEE 802.22 WRAN. In this paper, we consider the ATSC DTV signal, which is vestigial sideband (VSB) modulated. The proposed detection scheme is composed of two parts. The first is the DTV signal preprocessing part for the pilot tone of DTV signal filtering. The second part is the signal detector based on the Bussgang theorem. In the second part, we determine the existence of the DTV signal by applying the Bussgang theorem to the preprocessed input signal. A block diagram of the proposed detection scheme that includes the signal preprocessing block and the signal detection block is illustrated in Fig. 1.

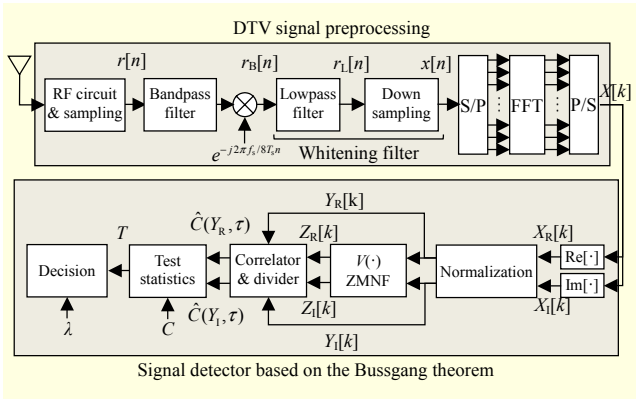

Fig. 1. Block diagram of proposed detection scheme.

1. DTV Signal Preprocessing

In the signal preprocessing block, the received signal is filtered using the bandwidth 6-MHz intermediate frequency (IF) bandpass filter and is down converted to place the frequency pilot tone at the baseband as

$$r_B[n] = \sum_{m=0}^{M_{IF}-1} h_{IF}[m] r[n-m] e^{-j2\pi f_p T_s n}, \quad (7)$$

where f_s depicts the sampling frequency, $h_{IF}[m]$ $(0 \le m \le M_{IF})$ is the IF bandpass filter, f_p represents the frequency of the pilot tone, T_s denotes the sample duration, and N is the number of the received sample. We filter $r_B[n]$ by the narrowband lowpass filter with bandwidth K/NT_s to obtain the frequency pilot, where K is the size of the fast Fourier transform (FFT). Then, the filtered frequency pilot is decimated by a factor of $N_d=N/K$. The filtered frequency pilot $r_L[n]$ and the decimated version $x[n]$ are described as

$$r_L[n] = \sum_{m=0}^{K_L-1} h_L[m] r_B[n-m], \quad 0 \le n < N, \quad (8)$$

$$x[n] = r_L[N_d n], \quad 0 \le n < K, \quad (9)$$

where $h_L[m]$ $(0 \le m \le M_L)$ is the lowpass filter for pilot filtering. The previous two steps are for the pilot filtering. Then, $x[n]$ is converted to the frequency domain signal $X[k]$ by using FFT as

$$X[k] = \sum_{n=0}^{K-1} x[n] e^{\frac{-j2\pi}{K} kn}, \quad 0 \le k < K. \quad (10)$$

After all these procedures, under the hypotheses H_0, both $x[n]$ and $X[k]$ are the stationary Gaussian signals. However, under the hypotheses H_1, $X[k]$ is not a stationary Gaussian signal due to the frequency pilot tone.

2. Proposed Detection Scheme

In the signal detector block of Fig. 1, the frequency domain pilot tone $X[k]$ is divided into the real and imaginary parts to apply the Bussgang theorem, $X_R[k] = \Re\{X[k]\}$ and $X_I[k] = \Im\{X[k]\}$. Each part is normalized to a zero-mean and unit variance with the sample mean and sample variance. Thus, $Y_R[k]$ is described as

$$Y_R[k] = \frac{X_R[k] - \hat{\mu}_{X_R}}{\hat{\sigma}_{X_R}}, \quad (11)$$

where $\hat{\mu}_{X_R}$ and $\hat{\sigma}^2_{X_R}$ are the estimated mean and variance of $X_R[k]$, respectively. $Y_I[k]$ can be obtained the same way. Since, $E\{X[k] \mid H_0\}$ is zero due to the down converting and the lowpass filtering, $\hat{\mu}_{X_R}$ and $\hat{\mu}_{X_I}$ can be removable. In this step, the proposed method does not use the noise variance but the variance of the received signal, so it is not related to the noise uncertainty. Noise uncertainty is caused by the difference between the estimated noise power and the real noise power in the received signal, and reducing the difference is not a simple problem. If there is a difference between the estimated variance of the received signal and the real one, we have a similar problem. However, the variance estimation of the received signal is a simple problem: $2\hat{\sigma}^2_{X_R} = 2\hat{\sigma}^2_{X_I} = \frac{1}{N}\sum_{n=0}^{N-1}(r[n] - \frac{1}{N}\sum_{n=0}^{N-1} r[n])^2$.

When the sensing time is 10 ms and 20 ms, the sample numbers are 215,040 and 430,080, respectively, and we can get the correct value. Note that the zero mean is the essential condition for the Bussgang theorem, but the unit variance is just for the simplicity of the system description. Furthermore, if the system contains an automatic gain controller, then the zero mean and the unit variance characteristic of the received signal can be obtained without an additional calculation.

After the normalization block, $Y_R[k]$ and $Y_I[k]$ pass through ZMNF, that is, $Z_R[k] = V\{Y_R[k]\}$ and $Z_I[k] = V\{Y_I[k]\}$. The sample proportionality constant is defined as

$$\hat{C}(A,\tau) = \frac{\frac{1}{K}\sum_{k=0}^{K-1} a[k]V(a[k+\tau])}{\frac{1}{K}\sum_{k=0}^{K-1} a[k]a[k+\tau]}, \quad (12)$$

where $A = \{a[0],\ldots,a[K-1]\}^T$ is the signal vector used for detection and τ is the time delay (–*K*, ..., *K*). The higher-order statistics-based method is a special case of the proposed method when ZMNF is the power series function, $V(x) = x^N$. If the input signal $a[k]$ is not the real Gaussian stationary process, then there is a difference between C and the sample proportionality constants. Therefore, we define the test statistic as

$$T = \sum_{\tau=-K}^{K} \{\hat{C}(Y_R,\tau) - C\}^2 + \{\hat{C}(Y_I,\tau) - C\}^2, \quad (13)$$

where $Y_R = \{Y_R[0],\ldots,Y_R[K-1]\}^T$ and $Y_I = \{Y_I[0],\ldots Y_I[K-1]\}^T$. Considering the detection device with multiple antennas, we redefine the test statistic as

$$T = \sum_{i=0}^{M-1} T_i, \quad (14)$$

where T_i is a test statistic from the *i*-th receiver using (13) and M is the number of antennas. Using the test statistics, we can decide whether the objective signal exists or not, as follows:

$$T \underset{H_0}{\overset{H_1}{\gtrless}} \lambda, \quad (15)$$

where λ is the predetermined threshold for ZMNF. The above equation states that if the test statistic $T \geq \lambda$, then PUS is present, and, if $T < \lambda$, then PUS is absent.

IV. Analysis on Threshold and Detection Probability

1. Detection Threshold

Analysis of the probability of the false alarm P_{FA} and the sensing threshold λ is discussed under the hypotheses H_0. The probability of the false alarm P_{FA} is generally given as the system requirement. The sensing threshold is determined as

$$\lambda = F_{T|H_0}^{-1}(1 - P_{FA}), \quad (16)$$

where $F_{T|H_0}(x)$ denotes the cumulative distribution function (CDF) of the test statistic under H_0.

To simplify the analysis, we assume no distortion is caused by the IF and lowpass filter. After the signal preprocessing steps, $Y_R[k]$ and $Y_I[k]$ are white Gaussian processes with $\mathcal{N}(0,1)$, so the autocorrelations of $Y_R[k]$ and $Y_I[k]$ are zero except for the case in which $\tau = 0$. Thus, we utilize only $\tau = 0$ for the DTV signal detection, and, for convenience, the time delay index will be omitted here. When $\tau = 0$, the denominator of (12) becomes 1 due to the normalization step. At this time, the sample proportionality constants under H_0 are represented as

$$\hat{C}(Y_R) = \frac{1}{K} Y_R^T Z_R \quad \text{and} \quad \hat{C}(Y_I) = \frac{1}{K} Y_I^T Z_I, \quad (17)$$

since $\frac{1}{K} Y_R^T Y_R = \frac{1}{K} Y_I^T Y_I = 1$. The sample proportionality constant is the sum of independent and identically distributed random variables. Based on the central limit theorem (CLT), each sample proportionality constant follows the Gaussian distribution with $\mathcal{N}(C, \sigma_0^2)$. The variance of the sample proportionality constant σ_0^2 is derived as follows:

$$\sigma_0^2 = \frac{1}{K}\left[E\left\{ (Y_R[k]Z_R[k])^2 \right\} - C^2 \right]. \quad (18)$$

In the above equation, $E\{(Y_R[k]Z_R[k])^2\}$ is determined by the ZMNF. For example, when $V(x) = x^n$, $E\{(Y_R[k]Z_R[k])^2\} = (2n+1)!!$, where $q!!$ denotes the double factorial, which is the product of every odd number from q to 1 and $n \geq 2$. Consequently, T is the sum of $2M$ squared Gaussian random variables with zero mean and variance σ_0^2. Therefore, it is distributed according to the central chi-squared distribution with $2M$ degrees of freedom. The CDF of T is described in the following:

$$F_{T|H_0}(x) = \int_0^x \frac{1}{\sigma_0^{2M} 2^M \Gamma(M)} u^{M-1} e^{-u/2\sigma_0^2} du, \quad (19)$$

where $\Gamma(\cdot)$ is the gamma function. For example, when M=1, the CDF of T is

$$F_{T|H_0}(x) = 1 - e^{-x/2\sigma_0^2}. \quad (20)$$

Using (16) and (20), the sensing threshold is derived as

$$\lambda = -2\sigma_0^2 \ln(P_{FA}). \quad (21)$$

The detection threshold of the proposed scheme is a function of M, P_{FA}, and σ_0^2 determined by ZMNF and K. The threshold does not require the noise power, so the proposed

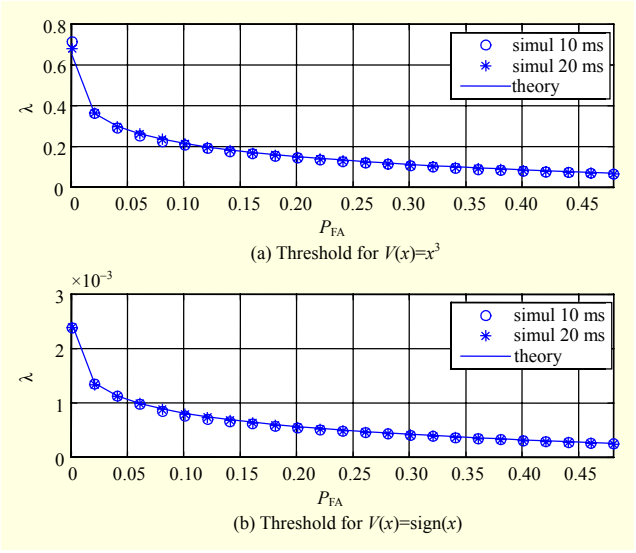

Fig. 2. Theoretical and numerical threshold vs. P_{FA} when (a) $V(x)=x^3$ and (b) $V(x)=\text{sign}(x)$, K=2,048, and M=1.

scheme is not affected by the noise uncertainty. Figure 2 describes the theoretical and numerical thresholds for the proposed scheme when M=1, K=2,048, and the sensing time is 10 ms and 20 ms. The used ZMNFs are x^3 and sign(x), which is the signum function. The threshold is not related to the sensing time, but we consider the sensing time for accuracy of the received power estimator.

2. Detection Probability

Analysis on P_D is treated under the hypotheses H_1. Derivation of the closed form of P_D is a very hard and complex problem since the exact modeling of the frequency pilot tone after the DTV signal preprocessing is difficult and the formulation of $F_{T|H_1}(x)$ is a hard problem. Therefore, we try to simplify the problem by using some reasonable assumptions, and we formulate P_D in AWGN.

First, we give the DTV signal model after the signal preprocessing as

$$X[k] = S[k] + \psi[k] + W[k], \tag{22}$$

where $S[k]$ and $\psi[k]$ respectively represent the filtered DTV signal part and pilot part in the frequency domain, and $W[k]$ denotes the complex AWGN with $\mathcal{CN}(0,\sigma_w^2)$. We divide the DTV signal into the signal part $S[k]$ and the pilot part $\psi[k]$. We can model $S[k]$ as $\mathcal{CN}(0,\sigma_s^2)$ because the bandwidth of the pilot filter is narrow, and the DTV signal follows Gaussian distribution. Then, $X[k]$ is rewritten as

$$X[k] = \psi[k] + \omega[k], \tag{23}$$

where $\omega[k] = W[k] + S[k]$ with $\mathcal{CN}(0,\sigma_s^2+\sigma_w^2)$. Considering the timing offset n_o and the frequency offset f_o within $\pm K/NT_s$, $\psi[k]$ is represented as

$$\psi[k] = a_p e^{j2\pi(f_p+f_o)T_s n_o} \frac{e^{j2\pi(f_o T_s N_d K-k)}-1}{e^{j2\pi(f_o T_s N_d K-k)/K}-1}, \tag{24}$$

where a_p denotes the pilot tone amplitude. The details of the pilot model are given in Appendix A. The sample means and variances of $X_R[k]$ and $X_I[k]$ for the large K are derived in Table 1. The means and the variances of $Y_R[k]$ and $Y_I[k]$ are also given in Table 1, where $\psi_R[k] = \Re\{\psi[k]\}$ and $\psi_I[k] = \Im\{\psi[k]\}$. The details of derivation of the means and the variances are given in Appendix B. When n_o and f_o are given, $\psi[k]$ is a deterministic signal, and $X[k]$ follows $\mathcal{CN}(\psi[k],\sigma_s^2+\sigma_w^2)$. This means that $X[k]$ is a nonstationary Gaussian signal.

Table 1. Means and variances.

Real part	Imaginary part
$\hat{\mu}_{X_R} \approx a_p \cos 2\pi(f_p+f_o)T_s n_o$	$\hat{\mu}_{X_I} \approx a_p \sin 2\pi(f_p+f_o)T_s n_o$
$\hat{\sigma}^2_{X_R} \approx \frac{1}{K}\sum_{k=0}^{K-1}\psi_R^2[k] - \hat{\mu}^2_{X_R} + \frac{\sigma_\omega^2+\sigma_s^2}{2}$	$\hat{\sigma}^2_{X_I} \approx \frac{1}{K}\sum_{k=0}^{K-1}\psi_I^2[k] - \hat{\mu}^2_{X_I} + \frac{\sigma_\omega^2+\sigma_s^2}{2}$
$\mu_{Y_R}[k] = (\psi_R[k] - \hat{\mu}_{X_R})/\hat{\sigma}_{X_R}$	$\mu_{Y_I}[k] = (\psi_I[k] - \hat{\mu}_{X_I})/\hat{\sigma}_{X_I}$
$\sigma^2_{Y_R}[k] = (\sigma_\omega^2+\sigma_s^2)/2\hat{\sigma}^2_{X_R}$	$\sigma^2_{Y_I}[k] = (\sigma_\omega^2+\sigma_s^2)/2\hat{\sigma}^2_{X_I}$

After passing ZMNF, the mean $\mu_{YZ}[k]$ and the variance $\sigma^2_{YZ}[k]$ of $Y_R[k]Z_R[k]$ and $Y_I[k]Z_I[k]$ are determined by ZMNF. When $V(x)=x^n$ for $n \geq 2$, $\mu_{YZ}[k] = E\{(Y_R[k])^{n+1}\} = E\{(Y_I[k])^{n+1}\}$ is the $(n+1)$th-order raw moment of $\mathcal{N}(\mu_Y[k],\sigma_Y^2[k])$, which can be represented by the central moments using the inverse binomial transform as follows [19]:

$$\begin{aligned}\mu_{YZ}[k] &= m'_{n+1}\left(\mu_Y[k],\sigma_Y^2[k]\right) \\ &= \sum_{a=0}^{n+1}\binom{n+1}{a} m_a\left(\sigma_Y[k]\right)^2 \left(\mu_Y[k]\right)^{n+1-a},\end{aligned} \tag{25}$$

where $m'_a(b,c)$ is the a-order raw moment of $\mathcal{N}(b,c)$ and $m_a(C)$ is the a-order central moment of $\mathcal{N}(0,c)$, that is,

$$m_a(\sigma_Y[k]) \begin{cases} 0, & a \text{ is odd}, \\ (a-1)!!(\sigma_Y[k])^a, & a \text{ is even}. \end{cases} \tag{26}$$

Then, $\sigma^2_{YZ}[k]$ for the $V(x)=x^n, n \geq 2$ is described as

$$\sigma^2_{YZ}[k] = m'_{2n+2}\left(\mu_Y[k],\sigma_Y^2[k]\right) - \mu^2_{YZ}[k]. \tag{27}$$

For another ZMNF $V(x)=\text{sign}(x)$, $\mu_{YZ}[k]$ is the first-order absolute moment of $\mathcal{N}(\mu_Y[k],\sigma_Y^2[k])$, and it is represented as

$$\mu_{YZ}[k] = \frac{1}{\sqrt{2\pi}\sigma_Y[k]} \int_{-\infty}^{\infty} |x| e^{-(x-\mu_Y[k])^2/2\sigma_Y^2[k]} dx$$
$$= \sqrt{\frac{2\sigma_Y^2[k]}{\pi}} e^{\frac{-\mu_Y^2[k]}{2\sigma_Y^2[k]}} + \mu_Y[k]\,\mathrm{erf}\left(\frac{\mu_Y[k]}{\sqrt{2}\sigma_Y[k]}\right), \quad (28)$$

where $\mathrm{erf}(\cdot)$ is the error function. The variance $\sigma_{YZ}^2[k]$ for $V(x)$=sign(x) can be easily obtained as

$$\sigma_{YZ}^2[k] = m_2'\left(\mu_Y[k], \sigma_Y^2[k]\right) - \mu_{YZ}^2[k]. \quad (29)$$

Under H_1, the sample proportionality constant is also a sum of K independent random variables with the mean $\mu_{YZ}[k]$ and variance $\sigma_{YZ}^2[k]$. Based on CLT, it is distributed according to $\mathcal{N}(\mu_1, \sigma_1^2)$, where $\mu_1 = \frac{1}{K}\sum_{k=0}^{K-1}\mu_{YZ}[k]$ and $\sigma_1^2 = \frac{1}{K^2}\sum_{k=0}^{K-1}\sigma_{YZ}^2[k]$. Then, T is the sum of the $2M$ squared Gaussian random variables:

$$T = \sum_{i=1}^{2M}(\hat{C}_i - C), \quad (30)$$

where $\hat{C}_i \sim \mathcal{N}(\mu_1[i], \sigma_1^2[i])$ is the proportionality constant obtained from the real and imaginary parts of M receivers. The sample proportionality constant under H_0 has the mean C and variance σ_0^2. By contrast, the sample proportionality constant under H_1 has a different mean $\mu_1[i]$ and variance $\sigma_1^2[i]$ due to the pilot tone. This difference makes the sensing scheme detect the DTV signal. In the special case $\psi_R[k] = \psi_1[k]$, which implies that $\mu_1[i] = \mu_1$ and $\sigma_1^2[i] = \sigma_1^2$, T is distributed according to the noncentral chi-square distribution with $2M$ degrees of freedom, which is a distribution of the sum of the $2M$ squared Gaussian random variables with $\mathcal{N}(\mu_1 - C, \sigma_1^2)$. The CDF of the test statistic under H_1 can be represented by using the M order generalized Marcum Q-function as [27]

$$F_{T|H_1}(x) = 1 - Q_M\left(s/\sigma_1, \sqrt{x}/\sigma_1\right), \quad (31)$$

where $s^2 = 2M(\mu_1 - C)^2$ is the noncentrality parameter of the chi-square distribution. Finally, P_D is derived as

$$P_D = Q_M\left(\sqrt{2M}\,|\mu_1 - C|/\sigma_1, \sqrt{-2\ln(P_{FA})}\sigma_0/\sigma_1\right). \quad (32)$$

3. Computational Complexity

The computational complexity of the proposed detection scheme can be divided into two parts, the DTV signal preprocessing part and the signal detection part. In the first part, most of the computations belong to the pilot filtering and FFT. Thus, $O(MN\log N + MK\log K)$ complex multiplications and additions are needed. The second part is the computation of a test statistic that includes the equations from (11) to (14). Without considering the complexity of ZMNF, $M(N+6K+12)$ multiplications and $M(3N+6K+3)$ additions are required. When $V(x)=x^n$, additional $2(n-1)KM$ multiplications are required. On the other hand, if $V(x)$=abs(x) or sign(x), then there is no additional complexity.

Table 2. Simulation parameters.

Parameters	Values
Over-sample rate	2
DTV signal bandwidth	6 MHz
Roll-off factor	0.115
Pilot amplitude a_p	1.25
Sampling frequency f_s	21.52 MHz
Intermediate frequency	5.38 MHz
Pilot frequency f_p	2.69 MHz
Probability false alarm P_{FA}	0.1
Number of FFT K	2,048
Number of receiver M	1 and 2
Sensing time NT_s	20 ms
Timing offset n_o	1,000 samples
Frequency offset f_o	1 kHz

V. Simulation Results

In this section, we will show the simulation results for the performance evaluation of the proposed sensing scheme by using the generated 8-VSB DTV signal based on [28] and [29] and the captured DTV signals in [26]. According to [30], the SNR is determined after the 6-MHz bandpass filter, and it is represented as

$$SNR = \frac{E\{|r_B[n]|^2|H_1\} - E\{|r_B[n]|^2|H_0\}}{E\{|r_B[n]|^2|H_0\}}. \quad (33)$$

Across the simulation results, the predetermined detection threshold is used for the given P_{FA}. The simulation parameters are described in Table 2. A raised cosine filter is used for the bandpass filter and the lowpass filter, and the roll-off factor is given in Table 2.

1. Generated DTV Signal Detection in AWGN

In this simulation, we provide the detection probability of the generated DTV signal in AWGN. According to the simulation

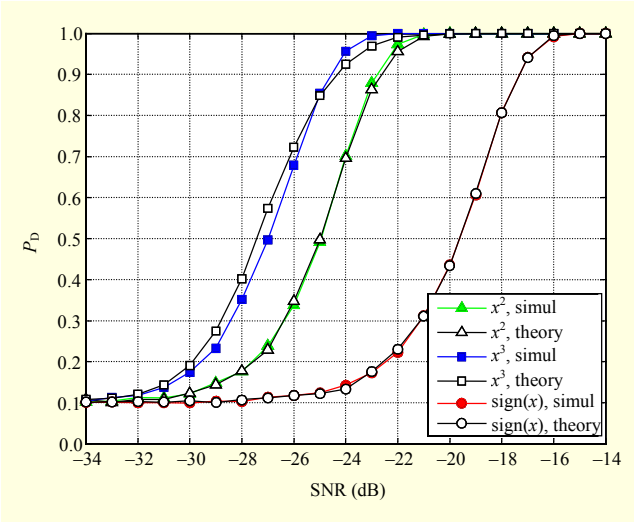

Fig. 3. Detection probability of proposed detection scheme in AWGN with single receiver M=1.

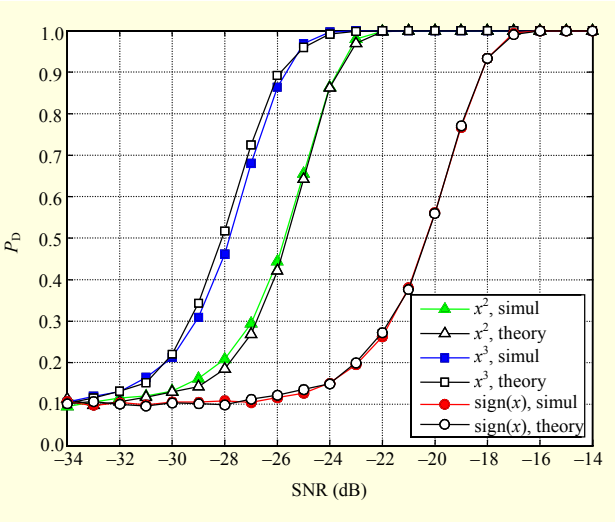

Fig. 4. Detection probability of proposed detection scheme in AWGN with multiple receivers M=2.

results presented in subsection IV.2, the analysis of P_D is verified, and we examine the impact of ZMNF and the number of receivers. By considering the DTV signal detector with a single receiver (M=1) and AWGN, the simulation result and the theoretical formulae described in subsection IV.1 are shown in Fig 3. Three kinds of ZMNFs are used ($V(x) = x^2$, x^3, and sign(x)), and the simulation curve and the analysis curve are marked "simul" and "theory," respectively.

As shown in Fig. 3, each ZMNF performs differently regarding detection, which is consistent with the results that are obtained through analysis. The proposed detection scheme can achieve P_D=0.9 under a –20-dB SNR when ZMNF x^2 and x^3 are used. Figure 4 gives the detection probability of the proposed scheme by considering multiple receivers (M=2). Increasing the number of receivers from 1 to 2, the required SNR to achieve P_D=0.9 is improved by 1 dB or 1.5 dB depending on the ZMNF. By comparing the simulation result to the theoretical result, we find that there are only a few differences between them. This difference is caused by certain assumptions that are used in our analysis. There is no distortion caused by bandpass filtering and lowpass filtering. The lowpass filtered DTV signal part is white Gaussian. $\hat{C}_i$ follows a Gaussian distribution based on CLT. However, the lowpass filtered DTV signal is not exactly white due to the raised cosine filter in the VSB modulation. Furthermore, when K is not large enough or the sample $Y[k]$ has a non-zero correlation, $\hat{C}_i$ does not follow Gaussian distribution. These reasons can create a difference between our analysis result and simulation result.

The Bussgang theorem holds for a stationary Gaussian process, so the proposed detection method can detect a nonstationary or non-Gaussian signal. In the analysis, $X[k]$ is a Gaussian signal, but it is a nonstationary signal due to the pilot tone. Therefore, the simulation results in Figs. 3 and 4 show the detection probability of the proposed signal when the PUS is a Gaussian signal.

2. Captured DTV Signal Detection

In this section, we evaluate the proposed scheme by using the captured DTV signals in [26]. From this simulation, we can see the impact of the frequency selective fading channel and the frequency offset that occurred in the practical detection environment. The initial signal processing of the captured DTV signal is based on [30], and we follow the simulation steps and the signal-sensing scenario 1 [31]. Among 51 captured DTV signals [26], we used the recommended 12 DTV signals in [31]. These signals were captured in Washington, DC, and each data sample collected was over 25 seconds long.

Figures 5 and 6 depict the detection performance of each DTV file with a single receiver, when $V(x)=x^3$ and $V(x)$=sign(x). There are significant differences in the detection performance among 12 DTV files, as each DTV signal has a different frequency offset and different amplitude of pilot tone caused by a multipath fading channel.

For comparison, we simulate the energy detector (ED) with the noise uncertainty and the eigenvalue-based detection methods, which is another detection scheme that overcomes the noise uncertainty. The threshold for ED uses the predetermined noise power, and the actual noise power is evenly distributed in the interval ±0.25 dB. The detection performance of ED is marked "ED 0.25 dB" and shown in Figs. 7 and 8. Simulation of the eigenvalue-based methods

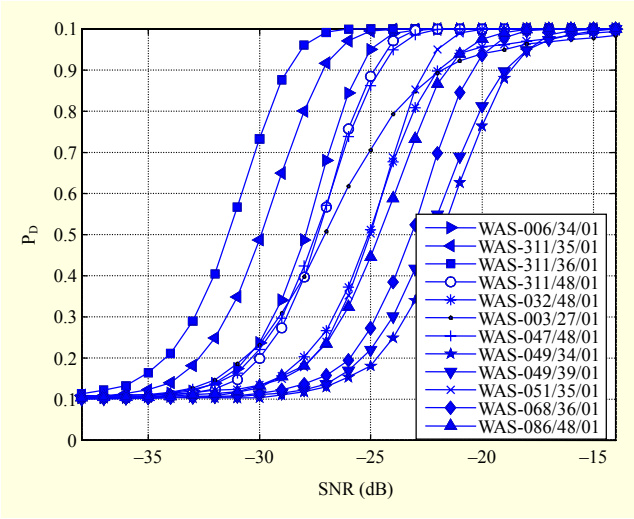

Fig. 5. Detection probability of proposed scheme with single receiver to detect each captured DTV signal when $V(x)=x^3$.

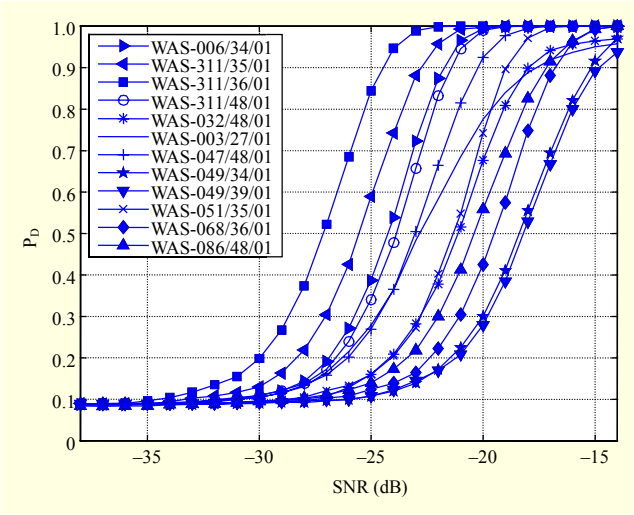

Fig. 6. Detection probability of proposed scheme with single receiver to detect each captured DTV signal when $V(x)=\text{sign}(x)$.

follows [32], and the respective decision for the maximum-minimum eigenvalue (MME) and the arithmetic-to-geometric mean (AGM) [33] is performed as

$$\frac{d_1}{d_L} \underset{H_0}{\overset{H_1}{\gtrless}} \lambda_{\text{MME}} \quad \text{and} \quad \frac{\frac{1}{L}\sum_{m=1}^{L} d_m}{\left(\prod_{m=1}^{L} d_m\right)^{1/L}} \underset{H_0}{\overset{H_1}{\gtrless}} \lambda_{\text{AGM}} \quad ,$$

where $\tilde{R}$ denotes the transformed sample covariance matrix, which is to compensate the impact of the bandpass filter, d_l denotes the l-th largest eigenvalue of $\tilde{R}$, L indicates the smoothing factor (the used L is 8), and λ_{MME} and λ_{AGM} are detection thresholds. Thresholds λ_{MME} and λ_{AGM} are adjusted to achieve the given P_{FA}. In MME and AGM, the bandpass

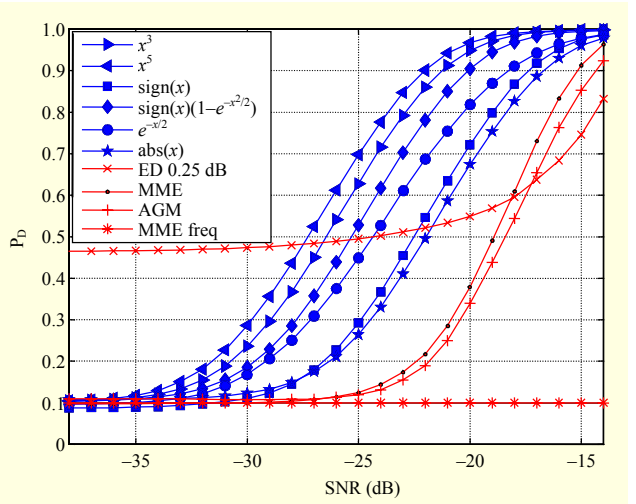

Fig. 7. Average detection probability over 12 captured DTV files with single receiver M=1.

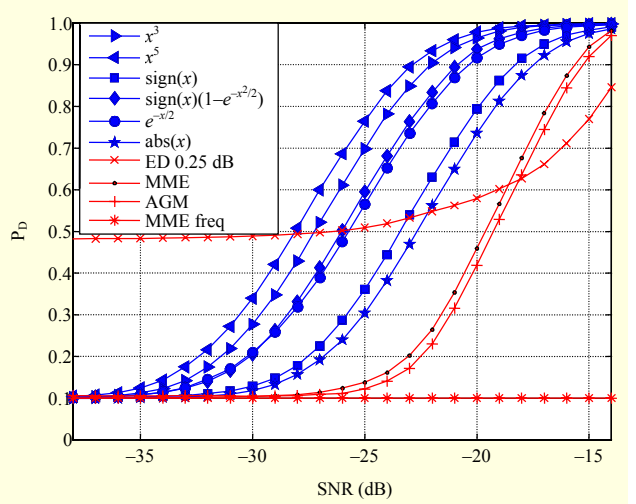

Fig. 8. Average detection probability over 12 captured DTV files with multiple receivers M=2.

filtered signal $r_{\text{B}}[n]$ is used to estimate the covariance matrix. To test the eigenvalue-based method using the frequency domain pilot signal, we evaluate the frequency domain MME that uses $X_{\text{R}}[k]$ and $X_{\text{I}}[k]$ to build the covariance matrix. In the eigenvalue-based method, the estimation of the covariance matrix is important, and it requires a large number of data samples to obtain the correct covariance matrix. When the sensing time is 20 ms, the number of the available data samples in the frequency domain is limited by the FFT size K, but it is about 200 times lower than N in the time domain. Therefore, the estimated covariance matrix in the frequency domain is inaccurate and the detection performance is not desirable.

The average detection performance of the proposed scheme over the 12 captured DTV files for variable ZMNF is given in

Figs. 7 and 8. The proposed algorithm using the three ZMNFs can achieve $P_D = 0.9$ subject to P_{FA}=0.1 under a –20-dB SNR with a single receiver. When the multiple receiver M=2 is used, we obtain about a 1.5-dB SNR gain. Most of the ZMNFs show much better performance than other methods. The sensing performance is also related to the specific ZMNF. The power series functions especially show desirable performance among the several ZMNFs that we evaluate in this simulation. When the higher- and odd-order power series function is used, the proposed algorithm achieves better sensing performance.

VI. Conclusion

This paper proposed the DTV signal detection scheme for the IEEE 802.22 WRAN system. The proposed scheme detects the DTV signal by using the Bussgang theorem. To detect the DTV signal, the proposed scheme detects the frequency domain pilot tone of the DTV signal. We also presented a mathematical analysis of the detection threshold and the detection performance in AWGN. The proposed detection scheme is unaffected by the noise uncertainty, and it shows desirable performance at a low SNR. ZMNF determines the detection performance and complexity, so it should be selected considering the system requirement. The proposed scheme can be employed in the detection of other signals as well as the DTV signal.

Appendix A. Frequency Domain DTV Pilot Model

If there is a symbol delay n_o and a frequency offset f_o, then the pilot part of $r[n]$ in AWGN is described as

$$r_p[n] = a_p e^{j2\pi(f_p+f_o)T_s(n+n_o)},$$

where n=0,…,N–1. Under the assumption that there is no distortion due to the IF filtering and lowpass filtering, the pilot part of $x[n]$ is

$$\begin{aligned} x_p[n] &= r_p[N_d n]e^{-j2\pi f_p T_s N_d n} \\ &= a_p e^{j2\pi(f_p+f_o)T_s n_o} e^{j2\pi f_o T_s N_d n}, \end{aligned}$$

where $n = 0,\ldots,K–1$. The frequency domain DTV pilot is

$$\begin{aligned} \psi[k] &= \sum_{n=0}^{K-1} x_p[n]e^{-j2\pi kn/K} \\ &= a_p e^{j2\pi(f_p+f_o)T_s n_o} \frac{e^{j2\pi(f_o T_s N_d K-k)}-1}{e^{j2\pi(f_o T_s N_d K-k)/K}-1}. \end{aligned}$$

Real and imaginary parts of $\psi[k]$ are written as

$$\psi_R[k] = \frac{a_p \sin\frac{\phi_2}{2}\cos(\phi_1 + \frac{K-1}{K}(\frac{\phi_2}{2}-\pi k))}{\sin\frac{1}{K}(\frac{\phi_2}{2}-\pi k)},$$

$$\psi_I[k] = \frac{a_p \sin\frac{\phi_2}{2}\sin(\phi_1 + \frac{K-1}{K}(\frac{\phi_2}{2}-\pi k))}{\sin\frac{1}{K}(\frac{\phi_2}{2}-\pi k)},$$

where $\phi_1 = 2\pi(f_p + f_o)T_s n_o$ and $\phi_2 = 2\pi f_o T_s N_d K$.

Appendix B. Means and Variances

1) Sample means of $X_R[k]$ and $X_I[k]$ are described as $\hat{\mu}_{X_R} = \Re\{x[0]\}$ and $\hat{\mu}_{X_I} = \Im\{x[0]\}$. For the large K, we estimate that $\hat{\mu}_{X_R} \approx E[\hat{\mu}_{X_R}] = \Re\{x_p[0]\}$ and $\hat{\mu}_{X_I} \approx E[\hat{\mu}_{X_I}] = \Im\{x_p[0]\}$. Finally, they are represented as

$$\hat{\mu}_{X_R} \approx a_p \cos\phi_1 \quad \text{and} \quad \hat{\mu}_{X_I} \approx a_p \sin\phi_1.$$

2) For the large K, sample variances of $X_R[k]$ and $X_I[k]$ are $\hat{\sigma}^2_{X_R} \approx E[\hat{\sigma}^2_{X_R}]$ and $\hat{\sigma}^2_{X_I} \approx E[\hat{\sigma}^2_{X_I}]$; therefore, these are rewritten as

$$\hat{\sigma}^2_{X_R} \approx \frac{1}{K}\sum_{k=0}^{K-1}\psi_R^2[k] - \hat{\mu}^2_{X_R} + \frac{\sigma_w^2+\sigma_s^2}{2},$$

$$\hat{\sigma}^2_{X_I} \approx \frac{1}{K}\sum_{k=0}^{K-1}\psi_I^2[k] - \hat{\mu}^2_{X_I} + \frac{\sigma_w^2+\sigma_s^2}{2}.$$

3) Means of $Y_R[k]$ and $Y_I[k]$ are $\mu_{Y_R} = E\{Y_R[k]\}$ and $\mu_{Y_I} = E\{Y_I[k]\}$, respectively, and they are represented as

$$\mu_{Y_R}[k] = \frac{\psi_R[k]-\hat{\mu}_{X_R}}{\hat{\sigma}_{X_R}} \quad \text{and} \quad \mu_{Y_I}[k] = \frac{\psi_I[k]-\hat{\mu}_{X_I}}{\hat{\sigma}_{X_I}}.$$

4) Variances of $Y_R[k]$ and $Y_I[k]$ are $\sigma^2_{Y_I} = E\{Y_I^2[k]\} - \mu^2_{Y_I}[k]$ and $\sigma^2_{Y_I} = E\{Y_I^2[k]\} - \mu^2_{Y_I}[k]$, respectively, and they are represented as $\sigma^2_{Y_R}[k] = \frac{\sigma_w^2+\sigma_s^2}{2\hat{\sigma}^2_{X_R}}$ and $\sigma^2_{Y_I}[k] = \frac{\sigma_w^2+\sigma_s^2}{2\hat{\sigma}^2_{X_R}}$.

References

[1] FCC, "Spectrum Policy Task Force Report," ET. Docket No. 02-155, Nov. 2002.

[2] J. Mitola and G.Q. Maguire, "Cognitive Radios: Making Software Radios More Personal," *IEEE Per. Commun.*, vol. 6, no. 4, Aug. 1999, pp. 13-18.

[3] C. Stevenson et al., "IEEE 802.22: The First Cognitive Radio Wireless Regional Area Network Standard," *IEEE Commun. Mag.*, vol. 47, no. 1, Jan. 2009, pp. 130-138.

[4] T. Yucek and H. Arslan, "A Survey of Spectrum Sensing Algorithms for Cognitive Radio Applications," *IEEE Commun. Surv. Tuts.*, vol. 11, no. 1, First Quarter 2009, pp. 116-130.

[5] S. Shellhammer, "Text on Energy Detector – For Informative Annex on Sensing Techniques," IEEE 802.22-07/0264r2, June 2007.

[6] H. Urkowitz, "Energy Detection of Unknown Deterministic Signals," *Proc. IEEE*, vol. 55, no. 4, Apr. 1967, pp. 523-531.
[7] S.M. Kay, *Fundamentals of Statistical Signal Processing: Detection Theory*, vol. 2, Prentice-Hall, 2003, pp. 439-526.
[8] S. Shellhammer and R. Tandra, "Performance of the Power Detector with Noise Uncertainty," IEEE 802.22-06/0134r0, July 2006.
[9] A. Mariani, A. Giorgetti, and M. Chiani, "Effects of Noise Power Estimation on Energy Detection for Cognitive Radio Applications," *IEEE Trans. Commun.*, vol. 59, no. 12, Dec. 2011, pp. 3410-3420.
[10] R. Tandra and A. Sahai, "SNR Walls for Signal Detection," *IEEE J. Sel. Topics Signal Process.*, vol. 2, no. 1, Feb. 2008, pp. 4-17.
[11] H.-S. Chen, W. Gao, and D.G. Daut, "Signature Based Spectrum Sensing Algorithms for IEEE 802.22 WRAN," *Proc. IEEE ICC*, June 2007, pp. 6487-6492.
[12] D. Bhargavi and C. Murthy, "Performance Comparison of Energy, Matched-Filter and Cyclostationarity-Based Spectrum Sensing," *Proc. IEEE Int. Works. SPAWC*, June 2010, pp. 1-5.
[13] H.-S. Chen, W. Gao, and D.G. Daut, "Spectrum Sensing Using Cyclostationary Properties and Application to IEEE 80.22 WRAN," *Proc. IEEE GLOBECOM*, Nov. 2007, pp. 3133-3138.
[14] B. Deepa, A.P. Iyer, and C.R. Murthy, "Cyclostationary-Based Architectures for Spectrum Sensing in IEEE 802.22 WRAN," *Proc. IEEE GLOBECOM*, Dec. 2010, pp. 1-5.
[15] W.A. Gardner, "Exploitation of Spectral Redundancy in Cyclostationary Signals," *IEEE Signal Process. Mag.*, vol. 8, no. 2, Apr. 1991, pp. 14-36.
[16] W.A. Gardner, "Spectral Correlation of Modulated Signals: Part I — Analog Modulation," *IEEE Trans. Commun.*, vol. 35, no. 6, June 1987, pp. 584-594.
[17] Y. Zeng and Y.-C. Liang, "Spectrum-Sensing Algorithms for Cognitive Radio Based on Statistical Covariances," *IEEE Trans. Veh. Technol.*, vol. 58, no. 4, May 2009, pp. 1804-1815.
[18] Y. Zeng and Y.-C. Liang, "Eigenvalue-Based Spectrum Sensing Algorithms for Cognitive Radio," *IEEE Trans. Commun.*, vol. 57, no. 6, June 2009, pp. 1784-1793.
[19] A. Papoulis and S.U. Pillai, *Probability, Random Variables and Stochastic Processes*, 4th ed., New York: McGraw-Hill, 2002.
[20] J.J. Bussgang, "Cross-Correlation Function of Amplitude-Distorted Gaussian Signals," Res. Lab. Elec., MIT, Cambridge, MA, Tech. Rep. 216, Mar. 1952.
[21] G. Giunta, G. Jacovitti, and G. Scarano, "Bussgang Gaussianity Test for Stationary Series," *Proc. IEEE SPW-HOS*, 1997, pp. 434-437.
[22] S. Shellhammer and R. Tandra, "An Evaluation of DTV Pilot Power Detection," IEEE 802.22-06/0188r0, Sept. 2006.
[23] D. Cabric, A. Tkachenko, and R.W. Brodersen, "Spectrum Sensing Measurements of Pilot, Energy, and Collaborative Detection," *Proc. IEEE MILCOM*, 2006, pp. 1-7.
[24] N. Kundargi and A. Tewfik, "Sequential Pilot Sensing of ATSC Signals in IEEE 802.22 Cognitive Radio Networks," *Proc. ICASSP*, 2008, pp. 2789-2792.
[25] C. Cordeiro et al., "Spectrum Sensing for Dynamic Spectrum Access of TV Bands," *Proc. CrownCom*, 2007, pp. 225-233.
[26] V. Tawil, 51 captured DTV signal, May 2006, http://grouper.ieee.org/groups/802/22
[27] J.G. Proakis and M. Salehi, *Digital Communications*, 5th ed., New York: McGraw-Hill, 2008, pp. 46-48.
[28] ATSC, "ATSC Digital Television Standard," ATSC Doc. A/53D, July 19, 2005.
[29] ATSC, "Guide to the Use of ATSC Digital Television Standard," ATSC Doc. A/54A, Dec. 4, 2003.
[30] S. Mathur et al., "Initial Signal Processing of Captured DTV Signals for Evaluation of Sensing Algorithm," IEEE 802.22-06/0158r5, Sept. 2006.
[31] S. Shellhammer et al., "Spectrum Sensing Simulation Model," IEEE 802.22-06/0028r10, Sept. 2006.
[32] Y. Zeng and Y.-C. Liang, "Text on Eigenvalue Based Sensing," IEEE 802.22-07/0297r1, July 2007.
[33] T.J. Lim et al., "GLRT-Based Spectrum Sensing for Cognitive Radio," *Proc. IEEE GLOBECOM*, 2008, pp. 1-5.

Sung Sue Hwang received his BS from the Department of Electrical and Computer Engineering, Pusan National University (PNU), Busan, Rep. of Korea, in 2007 and his MS from the Department of Electronics Engineering, PNU, in 2009. He is currently working toward his PhD in the Department of Electronics Engineering, PNU. His research interests include signal detection, channel estimation, wireless communication systems, and signal processing.

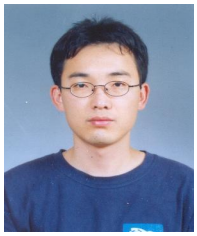

Dong Chan Park received his BS in electrical engineering and his MS in electronics engineering from Pusan National University (PNU), Busan, Rep. of Korea, in 2001 and 2004, respectively. He is currently working toward his PhD in the Department of Electronics Engineering, PNU. His research interests include distributed scheduling and interference management in wireless mesh networks.

Suk Chan Kim received his BS from the Department of Electronics Engineering, Pusan National University (PNU), Busan, Rep. of Korea, in 1993 and his MS and PhD in Electrical Engineering from the Korea Advanced Institute of Science and Technology (KAIST), Daejeon, Rep. of Korea, in 1995 and 2000, respectively. He was a teaching and research assistant at the Department of Electrical Engineering, KAIST, from 1993 to 1999 and a post-doctoral researcher for ETRI, Princeton University, and Lehigh University, from 2000 to 2001. He is now a professor in the Department of Electronics Engineering, PNU. He is a member of the Research Institute of Computer, Information, and Communication (RICIC), a member of the Institute of Electronics Engineering of Korea (IEEK), and a senior member of the Korean Institute of Electrical and Electronics Engineers (IEEE). His research interests include mobile communications, statistical signal processing, and communication networks.